Performance simulation of multi-row dry (and/or wet) heat exchangers

Elmahdy, A. H.; Biggs, R. C.

Publisher's version / Version de l'éditeur:

Proceedings, Sixth International Heat Transfer Conference: 1978-08, Toronto, Ontario, Canada, 4, pp. 327-332, 1978-01-01

National Research Council Canada
Conseil national de recherches Canada

PERFORMANCE SIMULATION OF MULTI-ROW DRY (AND / OR WET) HEAT EXCHANGERS

by A.H. Elmahdy and R.C. Biggs

Reprinted from
Volume 4, Preprints of papers presented at the
Sixth International Heat Transfer Conference
held in Toronto, 7 - 11 August 1978
p. 327 - 332

DBR Paper No. 797
Division of Building Research

Price 10 cents OTTAWA NRCC 16972

SOMMAIRE

On a mis au point un modèle mathématique qui sert à simuler le fonctionnement individuel des tubes d'un échangeur de chaleur à tubes à ailettes (serpentin) durant les procédés de refroidissement ou de refroidissement et de déshumidification. En résolvant numériquement le modèle, on peut obtenir les températures de l'air, de l'eau et de la surface des tubes ainsi que l'humidité spécifique de l'air pour chaque rangée de tubes du serpentin. Le coefficient moyen de transmission thermique du côté entrée d'air est calculé à l'aide d'une formule empirique qui met en relation le facteur J de la transmission thermique moyenne et le nombre de Reynolds pour le côté entrée d'air. Les résultats d'essais et d'analyses (conditions de l'air évacué et de l'eau, taux de chaleur sensible et latente) sur des serpentins à quatre et huit rangées se sont révélés compatibles durant les étapes de refroidissement et de déshumidification. Le modèle peut aussi servir d'algorithme pour la simulation du fonctionnement du serpentin; cette fonction fait d'ailleurs partie intégrante de programmes-machine mis au point pour effectuer des analyses de consommation d'énergie dans les réseaux de CVCA des bâtiments.

PERFORMANCE SIMULATION OF MULTI-ROW DRY (AND / OR WET) HEAT EXCHANGERS

A.H. Elmahdy[1]

R.C. Biggs[2]

1. National Research Council of Canada, Ottawa, K1A OR6
2. Canada Department of Public Works, Ottawa, K1A OM2

ABSTRACT

A mathematical model is developed to perform row-by-row simulation of finned-tube heat exchangers during cooling or cooling and dehumidification processes. Numerical solution of this model gives the air, water and tube surface temperatures and the air specific humidity after each row of tubes along the coil depth. The average heat transfer coefficient on the air side is calculated using an empirical formula that relates the average heat transfer J-factor with the air-side Reynolds number. Experimental and analytical results (outlet air and water conditions, sensible and latent heat rates) of 4- and 8-row coils showed good agreement during both cooling or cooling and dehumidification processes. This model can be used as an algorithm for coil performance simulation, which represents a part of general computer programs used for conducting energy analysis on HVAC systems in buildings.

NOMENCLATURE

A = area, m^2

A' = area per unit length in the direction of flow of air, m

A_m = minimum flow area, m^2

a and b = constants

C_1, C_2 = heat exchanger parameters

c = specific heat, J/kgK

c_p = specific heat of air at constant pressure, J/kgK

D_h = hydraulic diameter, m

E = energy, J/kg

h = specific enthalpy, J/kg

Δh_v = specific latent heat of evaporation, J/kg

J = heat transfer J-factor

L = coil depth, m

Le = Lewis number

$\dot{M}$ = mass flow rate, kg/s

$\dot{m}$ = mass flow rate per unit area, kg/m^2s

m = mass in the direction of flow of air, kg/m

Nu = Nusselt number

Pr = Prandtl number

$\dot{Q}$ = heat flow rate, W

R = thermal resistance, mK/W

$\bar{R}$ = air gas constant, J/kgK

r = fin radius, m

S = fin thickness, m

T = temperature, K

t = time, s

u = specific internal energy, J/kg

v = velocity, m/s

W = specific humidity $g_w/g_{dry\ air}$

x = distance in the direction of flow of water, m

y = distance in the direction of flow of air, m

α = heat transfer coefficient, W/m^2K

β = mass transfer coefficient based on air specific humidity difference, kg/m^2s

γ = c_p/c_v ratio of specific heat

η = efficiency

λ = thermal conductivity of fin material W/mK

ϕ = function

Subscripts

a = air

c = condition of moisture condensation

f = fin

g = gas

o = external

ov = overall

p = primary

r = radius

s = sensible - secondary

st = saturation

t = condition on the tube surface

w = water

1 = condition entering the cooling coil

2 = condition leaving the cooling coil

INTRODUCTION

Finned-tube heat exchangers (coils) are extensively used in many industrial applications where heat is to be transferred from one medium to another without being mixed. In air-conditioning systems, such multi-row (two or more) heat exchangers are generally used for heating or cooling the building air.

The thermal performance of these coils depends on many factors particularly the physical dimensions and arrangement of tubes and fins as well as the inlet conditions of the two media (in this case, moist air and chilled water). With heating coils, only sensible heat is transferred through the tube wall, and thus the design procedure and the prediction of coil performance is relatively easy compared with cooling and dehumidifying coils. With these last-mentioned coils, sensible and latent heat transfer occur simultaneously depending on the air dewpoint temperature and the chilled water temperature at the inlet to the coil. Added to these heat transfer mechanisms is the unpredictable flow pattern over different types of tube banks which makes an analytical solution of such flow (1) virtually impossible. This lack of knowledge of the coil characteristic has resulted in an over-design by as much as 100 per cent (2).

This paper presents a model that can be used to perform row-by-row numerical simulation of multi-row coils during simultaneous heat and mass transfer. Results from the analytical model are compared with some experimental results of tests on two heat exchangers (4 and 8 rows).

MATHEMATICAL MODEL

The purpose of this analysis is to predict the air temperature and humidity, and the temperature of the chilled water when leaving the cooling coil as well as the sensible and latent heat transfer rates for the given inlet conditions of the two fluids. This analysis can be applied to any type of finned tube heat exchanger provided the variation of the film heat transfer coefficient on the air side of the coil is known as a function of the air Reynolds number. The efficiency of the extended surface (fins) must also be known especially when cooling and dehumidifying occur. Figure 1 is a schematic diagram of a finned tube heat exchanger, where

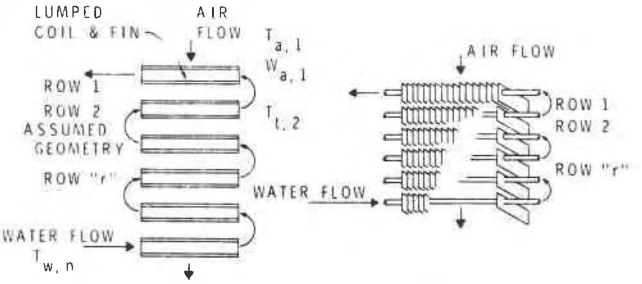

Figure 1. Cooling coil arrangement

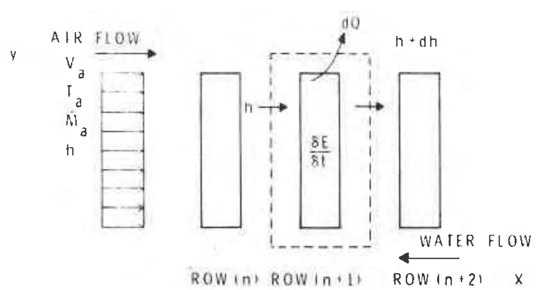

Figure 2. Increment of an air-coil area

moist air is in cross-counter flow with chilled water. At steady state conditions, a heat and mass balance on the control volume (Fig. 2) leads to the following equations:

$$\frac{dT_a}{dy} = \frac{-\eta_{s,o}}{R_a M_a c_p} (T_a - T_{t,o}) \tag{1}$$

$$\frac{dW_a}{dy} = \frac{-\eta_{c,o}}{M_a \, Le \, R_a c_p} (W_a - W_{t,o,st}) \tag{2}$$

$$\frac{dT_w}{dx} = \frac{-1}{M_w R_w c_w} (T_w - T_{t,o}) \tag{3}$$

$$T_{t,o} = R_x \{T_a + T_w \frac{R_a}{R_w \eta_{s,o}} + \frac{\eta_{c,o} h_g}{Le \, c_p \eta_{s,o}} (W_a - W_{t,o,st})\} \tag{4}$$

Also, it is assumed that:

$$W_{t,o,st} = a_1 + a_2 T_{t,o} + a_3 T_{t,o}^2 \tag{5}$$

where

$$R_x = \frac{R_w \eta_{s,o}}{R_a + R_w \eta_{s,o}} \tag{6}$$

a_1, a_2 and a_3 = constants

Equations (1) through (5) are solved simultaneously for the air dry-bulb temperature, T_a, water temperature, T_w, average outside tube surface temperature, $T_{t,o}$, air specific humidity, W_a, and saturated air specific humidity, at temperature $T_{t,o}$, $W_{t,o,st}$. The finite difference method is used to solve the differential equations, when the left-hand sides of Eqs. (1), (2) and (3) are replaced by $\frac{\Delta T_a}{\Delta y}$, $\frac{\Delta W_a}{\Delta y}$ and $\frac{\Delta T_w}{\Delta x}$ respectively. A detailed derivation of Eqs. (1) through (4) is given in Appendix A. Determination of the quantities $\eta_{s,o}$ and $\eta_{c,o}$ is obtained, first by solving the following equation to determine the temperature distribution over the fin surface during heat and mass transfer (3):

$$r \frac{d^2T_f}{d r^2} + \frac{dT_f}{dr} - r \frac{2\alpha_{ov}}{\lambda S} \left[T_f + \frac{h_g}{Le \, c_p} \{a + b (T_f - T_a) - W_a\}\right] = 0 \tag{7}$$

then substituting into the following expressions which define η_s and η_c respectively (4, 5):

$$\eta_s = \frac{\int_{A_f} (T_f - T_a) \, dA_f}{(T_{t,o} - T_a) A_f} \tag{8}$$

and

$$\eta_c = \frac{\int_{A_f} (W_{r,st} - W_a)\, dA_f}{(W_{t,o,st} - W_a)\, A_f} \qquad (9)$$

and finally, the over-all extended surface heat exchanger efficiencies are defined as:

$$\eta_{s,o} = 1 - \frac{A_s}{A_o} (1 - \eta_s) \qquad (10)$$

and

$$\eta_{c,o} = 1 - \frac{A_s}{A_o} (1 - \eta_c) \qquad (11)$$

AIR-SIDE HEAT TRANSFER COEFFICIENT

The average heat transfer coefficient on the air side, α_{ov}, of a dry surface is calculated using the following expression (6):

$$\alpha_{ov} = J\, \dot{m}_a\, c_p\, Pr^{-2/3} \qquad (12)$$

In Eq. (12), the maximum air mass flux, $\dot{m}_a$, is based on the minimum area of flow; the average heat transfer J-factor is defined as:

$$J = C_1\, Re^{C_2} \qquad (13)$$

Quantities C_1 and C_2 are constants for a particular coil and are strongly dependent on the tube arrangement and the physical dimensions of the heat exchanger. Reference 7 gives an analysis for evaluating C_1 and C_2 for staggered or inline circular tubes with circular or continuous flat fins with uniform thickness.

WATER-SIDE HEAT TRANSFER COEFFICIENT

The average film heat transfer coefficient on the water side, α_w, is evaluated using the turbulent flow relation (8):

$$Nu_w = 0.023\, Re_w^{0.8} Pr_w^{0.4} \qquad (14)$$

Equation (14) may underestimate α_w for the first row of the coil by 5 to 10%, since the flow is not fully developed. This does not result in a serious error, however, since the water-side thermal resistance represents only about 16 to 25% of the total resistance of heat flow for air Re between about 200 and 2000, and $Re_w > 3100$.

NUMERICAL SOLUTION OF STEADY STATE MODEL

Equations (1) through (5) are solved numerically using a finite differences technique. Because of the cross-counter flow arrangement, a value is assumed for the outlet water temperature, then the calculation proceeds in the direction of flow of air. The program checks on the coil surface condition at each row by comparing the air dewpoint temperature with the coil surface temperature. Having determined whether the coil surface is dry or wet, the calculations are directed to the appropriate subprograms. This is repeated row after row to the last row of the coil where the calculated chilled water temperature is compared with the given inlet temperature. If the difference is within the allowable limits, the execution is terminated, otherwise another iteration is necessary.

EXPERIMENTAL VERIFICATION

Four- and eight-row finned tube coils have been tested; a description of the test facility and procedure has been published (9). These coils have circular tubes, in a staggered arrangement, with continuous flat plate fins. A summary of the pertinent data is given in Table 1; Figure 3 shows the tube arrangement and some related dimensions.

TABLE 1 Summary of the Physical Data of the Coils Tested

	4-row	8-row
Face area, m^2	0.372	0.372
Minimum flow area/frontal area	0.54	0.54
Number of water circuits	16	16
Coil depth, m	0.14	0.29
Primary surface area, m^2	1.8	3.5
Secondary surface area, m^2	38.4	76.9

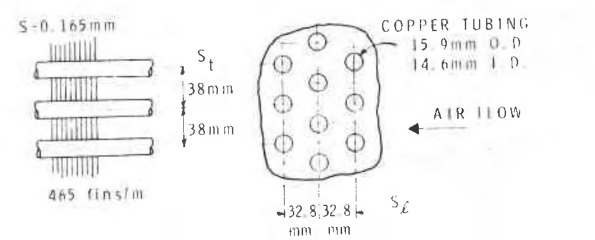

Figure 3. Physical dimensions of coil

In the experiments to perform sensible cooling and cooling and dehumidification of moist air: air Reynolds number, based on the coil hydraulic diameter, was varied between about 200 and 2000 (the coil hydraulic diameter is defined (6) as: $D_h = 4 \frac{A_m}{A_o} L$); air dry-bulb temperature was varied between 20 and 38°C; air relative humidity ranged between 20 and 80%; and air force velocity was varied between 1 and 5 m/s.

RESULTS

This algorithm was used to simulate the performance of multi-row finned tube heat exchangers. The results are compared with the corresponding experimental data obtained by testing two finned tube coils, as already described. The experimental

TABLE 2 Summary of Experimental and Analytical Results of 4-Row Coil*

Test No.	v_a	$T_{a,1}$ °C	$W_{a,1}$	$T_{w,1}$ °C	$T_{a,2}$ °C		$W_{a,2}$		$T_{w,2}$ °C		$\dot{Q}$	
					Exp	Analy	Exp	Analy	Exp	Analy	Exp	Analy
1-A	0.92	34.9	.0073	8.4	11.2	11.3	.0073	.0073	10.2	10.2	9376.	9405.
2-A	2.77	29.9	.0079	8.4	15.8	16.2	.0079	.0079	10.3	10.3	17931.	18166.
3-A	0.90	24.7	.0069	8.4	10.3	10.2	.0069	.0069	9.5	9.5	5742.	5772.
4-A	3.5	32.7	.0162	8.5	21.3	21.7	.0140	.0142	13.5	13.3	25813.	25373.
5-A	4.3	28.4	.0148	8.5	19.9	19.9	.0130	.0133	13.1	12.8	24963.	24465.
6-A	3.1	24.8	.0136	8.4	17.4	17.4	.0113	.0115	12.1	11.8	19162.	18781.

* Tests No. 1-A, 2-A, and 3-A are dry surface tests.
Tests No. 4-A, 5-A, and 6-A are wet surface tests.

TABLE 3 Summary of Experimental and Analytical Results of 8-Row Coil*

Test No.	v_a	$T_{a,1}$	$W_{a,1}$	$T_{w,1}$	$T_{a,2}$		$W_{a,2}$		$T_{w,2}$		$\dot{Q}$	
					Exp	Analy	Exp	Analy	Exp	Analy	Exp.	Analy
1-B	2.0	34.2	.0075	8.2	10.4	9.9	.0075	.0075	10.8	10.8	21711.	21711.
2-B	3.6	27.0	.0065	8.2	11.9	11.6	.0065	.0065	11.2	11.2	25022.	25081.
3-B	3.5	17.7	.0061	8.2	10.2	10.2	.0061	.0061	9.8	9.8	12687.	12745.
4-B	1.5	33.9	.0168	8.2	11.1	11.3	.0081	.0082	11.9	11.8	29974.	30179.
5-B	2.2	26.8	.0093	8.3	10.8	10.7	.0077	.0079	10.8	10.8	20598.	20305.
6-B	3.2	21.3	.0125	8.2	12.3	12.4	.0086	.0089	11.4	11.4	26370.	25872.

* Tests No. 1-B, 2-B, and 3-B are dry surface tests.
Tests No. 4-B, 5-B, and 6-B are wet surface tests.

results are given in Reference 9; a sample is presented here for comparison purposes. Test results of the 4- and 8-row coils, respectively, during dry cooling and cooling and humidification are summarized in Tables 2 and 3. Figure 4 shows the condition (or process) lines of the 4-row coil as plotted on a psychrometric chart. Test 1-A represents sensible cooling; tests 4-A, 5-A and 6-A are cooling and dehumidifying of moist air at different loading conditions. Similarly, in the case of the 8-row coil, sensible cooling and combined sensible latent cooling of moist air are represented by tests 1-B (sensible cooling), 4-B, 5-B and 6-B on the psychrometric chart (Figure 5).

DISCUSSION

During sensible cooling of moist air, the condition (or process) line is simply a straight horizontal line, as it appears on the psychrometric chart (see tests 3-A and 1-B in Figures 4 and 5 respectively). On the other hand, in the cooling and dehumidification of moist air, the process line droops as it approaches the saturation line (see tests 4-A, 5-A and 6-A in Figure 4 and tests 4-B, 5-B and 6-B in Figure 5). The dashed lines on these figures represent the predicted condition lines of the two coils during different loading conditions. Comparison between experimentally determined and analytically predicted air temperature and specific humidity,

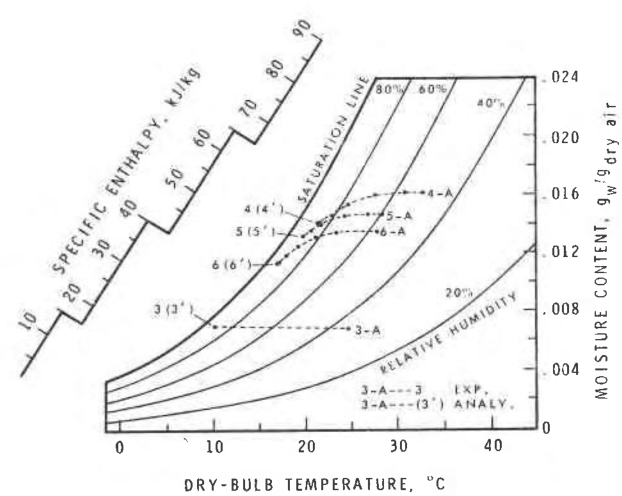

Figure 4. Condition line of the 4-row coil during cooling and cooling and dehumidification (Tests Nos. 3, 4, 5 and 6 of Table 2).

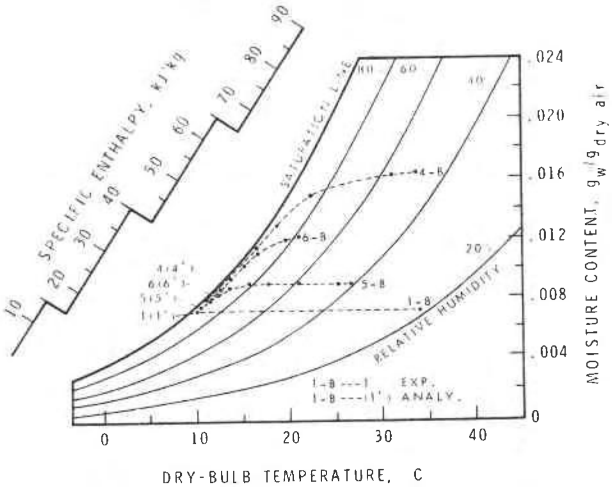

Figure 5. Condition line of the 8-row coil during cooling and cooling and dehumidification (Tests Nos. 1, 4, 5 and 6 of Table 3).

water temperature and cooling load is given in Tables 2 and 3 for the 4- and 8-row coils respectively. Agreement between the corresponding quantities is within experimental uncertainty. For example, the maximum difference between the measured and predicted air dry-bulb temperature is about 0.5°C; the difference in the temperature of the leaving chilled water is less. Although the algorithm of coil performance simulation predicts the psychrometric conditions of the moist air and chilled water as they pass through the heat exchanger, no attempt was made to check these intermediate results. The close comparison between the leaving actual and leaving predicted conditions of the two media are believed to be sufficient to validate the model presented in this paper.

REFERENCES

1. Eckert, E.R.G., and Drake, R.M. Jr. Analysis of Heat and Mass Transfer, McGraw-Hill Co., 1972
2. Sabersky, R.H., Heat Transfer in the Seventies, Int. Journal of Heat and Mass Transfer, Vol. 14, p. 1927-49, 1971
3. Elmahdy, A.H., and Biggs, R.C., Efficiency of Extended Surfaces with Simultaneous Heat and Mass Transfer, (In process)
4. Ware, C., and Hacha, T., Heat Transfer from Humid Air to Fin and Tube Extended Surface Cooling Coils, ASME Paper No. 60-Ht-17
5. O'Brien, N.G., and Turner, R.L., Fin Thermal Efficiency During Simultaneous Heat and Mass Transfer, A.I.Ch.E. Journal, Vol. 11, No. 3, p. 546-548, 1965
6. Kays, W.M., and London, A.L., Compact Heat Exchangers, McGraw-Hill Co., 1964
7. Elmahdy, A.H., and Biggs, R.C., Finned Tube Heat Exchangers: Correlation of Dry Surface Heat Transfer Data. (In process)
8. McAdams, W.H., Heat Transmission, McGraw-Hill Co., 3rd Ed., p. 219, 1954
9. Elmahdy, A.H., and Mitalas, G.P., Facility for Testing Cooling and Dehumidifying Coils: Description, Procedures and Test Results. (In process)

APPENDIX A

DERIVATION OF THE MATHEMATICAL MODEL OF COOLING COIL PERFORMANCE SIMULATION

For completeness, a dynamic model is derived to simulate the thermal characteristic of multi-row finned tube heat exchangers. This model can be used for further studies related to the dynamic characteristics of heat exchangers, which in turn can be used in the study of automatic control associated with HVAC systems. Considering Figs. 1 and 2 of the main text, the following basic assumptions were made:

1. uniform conditions of moist air and chilled water at entry to the heat exchanger,
2. all the heat is transferred from the air stream to the chilled water (i.e., no heat loss to the surroundings),
3. the thermal capacity of the water film condensate is neglected (A1).
4. air is assumed to be completely mixed between rows (A2).

Energy balance on the incremental volume shown in Fig. 2 gives:

$$\dot{M}_a \, dh = \frac{\dot{M}_a}{v_a} \frac{\partial E}{\partial t} dy + d\dot{Q} \qquad \text{(A-1)}$$

The heat transfer, $d\dot{Q}$, is the sum of the sensible and latent heat transfer through the primary and secondary surfaces (bare tube and fin surfaces respectively):

$$d\dot{Q} = \{\int_{A'_f} \alpha (T_a - T_f) \, dA'_f + \int_{A'_f} \beta \Delta h_v \, (W_a - W_{f,st}) \, dA'_f + $$
$$+ \alpha A'_f \, (T_a - T_t) + \beta A'_p \, \Delta h_v \, (W_a - W_{t,st})\} \, dy \qquad \text{(A-2)}$$

Using the definition of heat exchanger efficiency as defined by Eqs. (8), (9), (10) and (11), Eq. (A-2) can be rearranged as:

$$d\dot{Q} = \{\alpha A'_o \, \eta_{s,o} \, (T_a - T_{t,o}) + $$
$$+ \beta \Delta h_v \, A'_o \, \eta_{c,o} \, (W_a - W_{t,o,st})\} \, dy \qquad \text{(A-3)}$$

Since the enthalpy of moist air can be expressed as (A1):

$$h = \phi \, (T_a, W_a) \qquad \text{(A-4)}$$

Therefore

$$\frac{\partial h_a}{\partial t} = c_p \frac{\partial T_a}{\partial t} + \Delta h_v \frac{\partial W_a}{\partial t} \qquad \text{(A-5)}$$

and

$$\frac{\partial h_a}{\partial y} = c_p \frac{\partial T_a}{\partial y} + \Delta h_v \frac{\partial W_a}{\partial y} \qquad \text{(A-6)}$$

Mass balance of moisture gives:

$$\frac{\dot{M}}{v_a} \frac{\partial W_a}{\partial t} + \dot{M}_a \frac{\partial W_a}{\partial y} = - \beta \, \eta_{c,o} \, A'_o \, (W_a - W_{t,o,st}) \qquad \text{(A-7)}$$

The change in stored energy E can be expressed as:

$$\frac{\partial E}{\partial t}\, dy = \frac{\partial u_a}{\partial t}\, dy \tag{A-8}$$

Substituting Eqs. (A-3), (A-5), (A-6) and (A-8) into Eq. (A-1):

$$- \alpha A'_o \eta_{s,o} (T_a - T_{t,o}) - \beta \Delta h A'_o \eta_{c,o} (W_a - W_{t,o,st}) = \dot{M}_a c_p \frac{\partial T_a}{\partial y} + \frac{M_a c_v}{v_a} \frac{\partial T_a}{\partial t} + \dot{M}_a \Delta h_v \frac{\partial W_a}{\partial} + \frac{\dot{M}_a}{v_a} u_g \frac{\partial W_a}{\partial y} \tag{A-9}$$

Note that Δh_v can be replaced by h_g at the same temperature, since the difference between Δh_v and h_g is very small when multiplied by W_a (A1). Rearrangement of Eqs. (A-7) and (A-9) results in:

$$\frac{\dot{M}_a}{v_a} c_v \frac{\partial T_a}{\partial t} + \dot{M}_a c_p \frac{\partial T_a}{\partial y} = (-\alpha A'_o \eta_{s,o} (T_a - T_{t,o}) + \frac{\dot{M}_a}{v_a} (h_g - u_g) \frac{\partial W_a}{\partial t} \tag{A-10}$$

Notice that:

$$h_g - u_g = \bar{R}\, T_a \tag{A-11}$$

If the Lewis number is introduced:

$$Le = \frac{\alpha}{\beta c_p} \tag{A-12}$$

Eq. (A-10) becomes:

$$\frac{\partial T_a}{\partial t} + \gamma v_a \frac{\partial T_a}{\partial y} = - \frac{\gamma \eta_{s,o}}{M_1 R_a} (T_a - T_{t,o}) + (\gamma - 1) T_a \frac{\partial W_a}{\partial t} \tag{A-13}$$

and Eq. (A-7) becomes:

$$\frac{\partial W_a}{\partial t} + v_a \frac{\partial W_a}{\partial y} = - \frac{\eta_{c,o}}{M_1\, Le\, R_a} (W_a - W_{t,o,st}) \tag{A-14}$$

where

$$M_1 = \frac{\dot{M}_a c_p}{v_a} \tag{A-15}$$

and

$$R_a = \frac{1}{\alpha A'_o} \tag{A-16}$$

Part of the heat transferred from the air is stored in the tube and fin material, therefore we can write:

$$\frac{\partial T_a}{\partial t} + \frac{\eta_s + \frac{m_t c_t}{m_f c_f}}{1 - \eta_s} \frac{\partial T_{t,o}}{\partial t} = \frac{\eta_{s,o} (T_a - T_{t,o})}{R_a (1 - \eta_s) m_f c_f} + \frac{\eta_{c,o} h_g (W_a - W_{t,o,st})}{m_f c_f\, Le\, R_a c_p (1 - \eta_s)} - \frac{T_{t,o} - T_w}{R_w c_f m_f (1 - \eta_s)} \tag{A-17}$$

where

$$R_w = \frac{1}{\alpha_i A'_{t,i}} \tag{A-18}$$

Heat balance on the chilled water yields:

$$\frac{\partial T_w}{\partial t} + v_w \frac{\partial T_w}{\partial x} = \frac{v_w}{R_w \dot{M}_w c_w} (T_{t,o} - T_w) \tag{A-19}$$

Finally, use Eq. (5) of the main text to calculate the specific humidity of saturated air at temperature, $T_{t,o}$.

Eq. (A-13), (A-14), (A-17), (A-19) and (5) represent the dynamic model to simulate the performance of a finned-tube multi-row heat exchanger. For purposes of this paper, the steady state model can be obtained by dropping the $(\frac{\partial}{\partial t})$ terms of the above equations. Therefore Eq. (A-13) becomes:

$$\frac{dT_a}{dy} = - \frac{\eta_{s,o}}{R_a \dot{M} c_p} (T_a - T_{t,o}) \tag{A-20}$$

Eq. (A-14) yields:

$$\frac{dW_a}{dy} = - \frac{\eta_{c,o}}{\dot{M}_a\, Le\, R_a c_p} (W_a - W_{t,o,st}) \tag{A-21}$$

Eq. (A-19) gives:

$$\frac{dT_w}{dx} = - \frac{1}{\dot{M}_w R_w c_w} (T_w - T_{t,o}) \tag{A-22}$$

and Eq. (A-17) becomes:

$$T_{t,o} = \frac{R_w \eta_{s,o}}{R_a + R_w \eta_{s,o}} \{T_a + T_w \frac{R_a}{R_w \eta_{s,o}} + \frac{\eta_{c,o} h_g (W_a - W_{t,o,st})}{Le\, c_p \eta_{s,o}}\} \tag{A-23}$$

Eqs. (A-20) through (A-23) and (5) can be solved numerically for T_a, W_a, T_w, $T_{t,o}$ and $W_{t,o,st}$ as described in the main text.

REFERENCES

A1 Threlkeld, J.L. Thermal Environmental Engineering, 2nd Ed., Prentice-Hall, Englewood Cliffs, N.J., 1970

A2 McCullagh, K.R., et al., An analysis of Chilled Water Cooling Dehumidifying Coils Using Dynamic Relationships, ASHRAE Trans., Vol. 75, Part II, 1969.